Stability and efficacy of synthetic cationic antimicrobial peptides nebulized using high frequency acoustic waves

Ying Wang,[1] Amgad R. Rezk,[2] Jasmeet Singh Khara,[1] Leslie Y. Yeo,[2,a)] and Pui Lai Rachel Ee[1,a)]
[1]*Department of Pharmacy, National University of Singapore, 18 Science Drive 4, Singapore, Singapore 117543*
[2]*Micro/Nanophysics Research Laboratory, School of Civil, Environmental and Chemical Engineering, RMIT University, Melbourne, Victoria 3000, Australia*

(Received 26 April 2016; accepted 26 May 2016; published online 7 June 2016)

Surface acoustic wave (SAW), a nanometer amplitude electroelastic wave generated and propagated on low-loss piezoelectric substrates (such as $LiNbO_3$), is an extremely efficient solid–fluid energy transfer mechanism. The present study explores the use of SAW nebulization as a solution for effective pulmonary peptide delivery. *In vitro* deposition characteristics of the nebulized peptides were determined using a Next Generation Cascade Impactor. 70% of the peptide-laden aerosols generated were within a size distribution favorable for deep lung distribution. The integrity of the nebulized peptides was found to be retained, as shown via mass spectrometry. The anti-mycobacterial activity of the nebulized peptides was found to be uncompromised compared with their non-nebulized counterparts, as demonstrated by the minimum inhibition concentration and the colony forming inhibition activity. The peptide concentration and volume recoveries for the SAW nebulizer were significantly higher than 90% and found to be insensitive to variation in the peptide sequences. These results demonstrate the potential of the SAW nebulization platform as an effective delivery system of therapeutic peptides through the respiratory tract to the deep lung. *Published by AIP Publishing.* [http://dx.doi.org/10.1063/1.4953548]

I. INTRODUCTION

In recent decades, the pivotal role of antimicrobial peptides (AMPs) in the treatment of infectious diseases,[1,2] in particular, pulmonary infections, has been reiterated by their ability to eliminate multidrug-resistant pathogens associated with lung disease including *Mycobacterium tuberculosis*, *Acinetobacter baumannii*, and *Pseudomonas aeruginosa*.[3–5] However, systemic peptide delivery is afflicted with problems including high susceptibility to enzymatic degradation, low permeability across biological membranes, and rapid clearance in blood, which have hampered the clinical application of AMPs for the therapeutic treatment of lung diseases.[6]

Inhalation drug delivery is an attractive alternative strategy for lung diseases as they offer high lung deposition concentration and low systemic toxicity.[7] Such needle-free inhalation-based therapies avoid first-pass metabolism and offer patients a painless user experience.[8] Thus, pulmonary delivery of peptides via inhalation using dry powder inhalers (DPIs) is being extensively explored for the treatment of both pulmonary and non-pulmonary diseases.[9–13] In addition, aerosolized AMPs are currently being incorporated into treatment regimens as a conjunctive therapy in patients with multi-drug resistant infection who are irresponsive to systemic therapy.[14]

[a)]Authors to whom correspondence should be addressed. Electronic addresses: leslie.yeo@rmit.edu.au and phaeplr@nus.edu.sg.

Pulmonary drug delivery devices generally fall into two categories: inhalers, which include metered dose inhalers (MDI) and dry powder inhalers (DPI), and nebulizers.[15] Inhalers require hand-breath coordination skills, which can be challenging for children, the elderly, and patients with compromised respiratory system.[15] For peptide delivery using dry powder inhalers, special excipients and pre-processing, such as micronization, are required to generate discrete particles for better flow characteristics and homogeneous distribution of peptides within the powder blend.[11,16] Conventional nebulizers, however, are limited by their large power requirements and sizes, which hinder portable use outside hospital settings, the tendency of their orifices to clog, and their propensity to denature macromolecules, such as the peptides considered in this work.[17]

Emerging from recent developments in SAW microfluidics,[18–22] SAW nebulizers[23,24] have been identified as a promising low cost alternative for conventional nebulizers,[25] in addition to other novel applications such as mass spectrometry (MS),[26–28] among others. They consume substantially less power (1 W) than conventional ultrasonic nebulizers (10–100 W),[24] therefore introducing considerable potential for miniaturization and thus portability. In addition, the risk of denaturing macromolecules is much lower because the considerably higher SAW frequencies (10–100 MHz) compared with the ultrasonic nebulizers (10 kHz–1 MHz), together with the significantly lower power input, suppress hydrodynamic shear and cavitation molecular damage.[29] In the present study, we set out to evaluate the potential utility of the SAW platform for therapeutic peptide nebulization in order to develop a low cost, non-invasive, and portable device for pulmonary delivery of therapeutic peptides.

Six model anti-mycobacterial peptides were selected for SAW nebulization (Table I). These peptides exhibit superior killing efficiencies against various mycobacterial strains and vary in amino acid sequence, charge, secondary conformation, and hydrophobicity,[30,31] thus facilitating the understanding of how various physiochemical parameters affect peptide nebulization. Our results showed that the nebulization process neither compromised peptide integrity nor anti-mycobacterial activity and highlight the potential of the SAW platform as an effective pulmonary delivery system for therapeutic peptides.

II. MATERIALS AND METHODS

A. Materials

Model peptides RR-11 (RKDVYRRRRRR), RY-11 (RRRRRRRKDVY), LK-8 ($LLKKLLKK_2$), MM-10 (MLLKKLLKKM), II-10 (ILLKKLLKKI), and WW-10 (WLLKKLLKKW) were custom synthesized using the Fmoc-solid phase protocol by GL Biochem (Shanghai, China) and their molecular weights were confirmed by matrix-assisted laser desorption/ionization time-of-flight mass spectroscopy (MALDI-TOF MS; Model 4800, Applied Biosystems, Grand Island, NY, USA). *Mycobacterium smegmatis* (ATCC No. 14468) was purchased from ATCC (American Type Culture Collection, Manassas, VA, USA), and

TABLE I. Peptide designs and molecular weight characterization. Close agreement between measured and theoretical molecular weights was observed.

Peptides	Peptides sequence	Theoretical M_W	Observed M_w[a]	Net charge	Hydrophobic composition (%)	Secondary structure
RR-11	RKDVYRRRRRR	1615.92	1616.02	+8	18	Random coil
RY-11	RRRRRRRKDVY	1615.92	1616.02	+8	18	Random coil
LK-8	LLKKLLKK	982.37	983.02	+5	60	α-helix
MM-10	MLLKKLLKKM	1244.76	1244.83	+5	60	α-helix
II-10	ILLKKLLKKI	1208.69	1209.15	+5	60	α-helix
WW-10	WLLKKLLKK	1354.80	1356.40	+5	60	α-helix

[a]Measured by MALDI-TOF MS, apparent $M_w = [M_W + H]^+$.

nutrient broth (Acumedia No. 7146) and bacteriological agar (Acumedia No. 7176) were purchased from Neogen Corporation (Lansing, MI, USA).

B. SAW device fabrication

SAW devices were fabricated by patterning focused interdigital transducer electrodes using standard photolithographic techniques previously described[32] on 127.86° YX rotated single crystal lithium niobate piezoelectric substrates (Roditi, London, UK). Briefly, we sputtered 5 nm of chromium followed by 1.5 μm of aluminum, followed by the spin coating of AZ1512 photoresist, UV exposure, and wet etching. The width and gap spacing of the electrodes are patterned in order to set the wavelength and hence the frequency of the device; in this work, an SAW frequency of 29.78 MHz is employed. The 10 nm amplitude SAW at this frequency is then generated on the device when a sinusoidal electric field is applied to the electrodes using a single-channel Arbitrary Function Generator (WS8351, Tabor Electronics, Tel Hanan, Israel) and amplifier (ZHL-5 W-1, 5–500 MHz, Mini Circuits, Brooklyn, NY, USA). Nebulization of the liquid then ensues when it is delivered to the surface of the device in the pathway of the SAW (Fig. 1(a)); the nebulization rate is optimized by ensuring that the liquid is delivered to the focal point of the focused SAW radiation, as illustrated in Fig. 1(b). Voltage and current probes were used to measure the power that was displayed on an oscilloscope (Wavejet 332/334, LeCroy, Chestnut Ridge, NY, USA). The measured power used in the experiments was fixed at 2.93 W.

C. Peptide nebulization and aerosol characterization

Peptide solutions in deionized (DI) water of fixed concentration (500 mg/l) were pipetted dropwise onto the SAW substrate and consequently nebulized in an enclosed Falcon tube as depicted in Fig. 1(a) at a rate of 3–5 ml/h. The condensate of the nebulized peptide mist was then collected for further analysis by centrifuging the tube at speed of 4000 rpm. The drop size distribution of the mist was characterized using a Next Generation Cascade Impactor (NGI; Copley Scientific Ltd., Nottingham, UK), which, schematically illustrated in Fig. 2, is the accepted US and European pharmaceutical industry standard *in vitro* model for examining airway particle deposition.[33,34] Briefly, the NGI draws the aerosol mist through the induction port under an imposed air flow, whose rate is set at standard accepted values prescribed by the

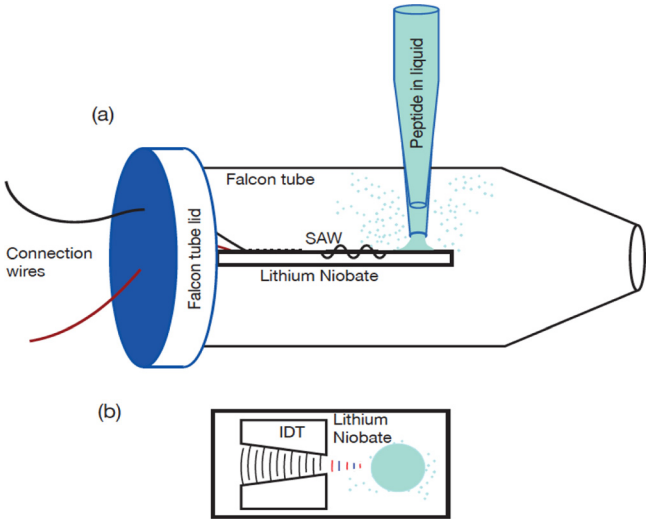

FIG. 1. Schematic illustration of (a) the experimental setup used in the SAW peptide nebulization studies. The entire SAW device was confined within a Falcon tube in order to facilitate collection of the nebulized peptide condensate. A pipette tip was positioned such that the peptide solution is delivered to the focal point of the focused SAW, as indicated in the top view schematic of the device in (b) to maximize the nebulization rate.

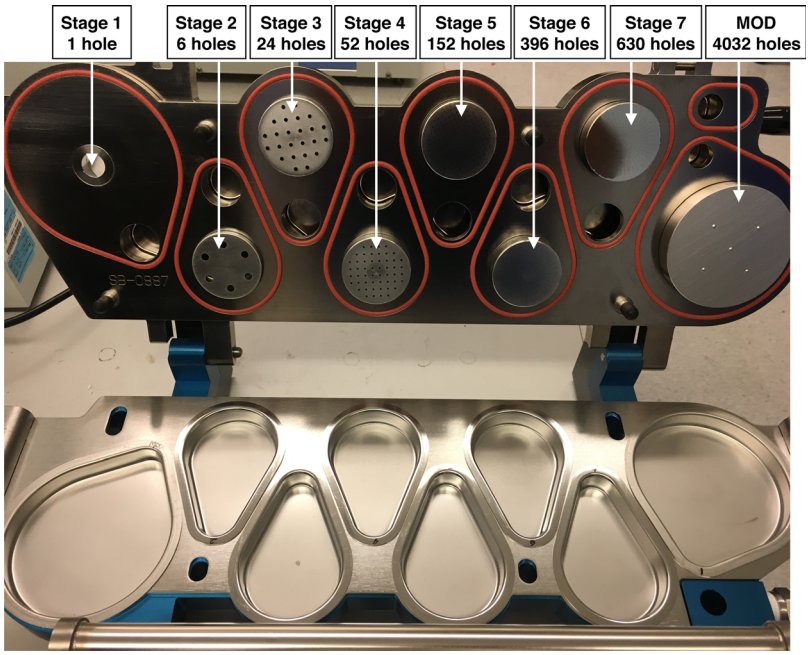

FIG. 2. Schematic illustration of an NGI, including working components and nozzle configuration.

pharmacopeia that have been determined to correspond closely with that of inspiratory flow during inhalation. The aerosol mist travels through seven stages with progressively decreasing orifice dimensions, thus fractionating the aerosols such that aerosol droplets with dimensions above a cut-off for a particular stage impact on the stage and are collected, whereas droplets with dimensions below the cut-off pass through onto the next stage. By ascertaining the mass and concentration of the liquid in the collection cups for each stage, it is then possible to determine the relative aerosol size fractions and hence obtain an approximation indication of the proportions of the liquid that are deposited in various parts of the lung (see, for example, Table II).

Here, 5 ml of WW-10 solution at 2 mg/ml was nebulized from the induction port, and the mist was introduced into the NGI under 50% relative humidity at a flow rate of 15 l/min, which mimics the inspiratory flow rate in adult tidal breathing.[35] We note that the aerosol size distribution to be sensitive only to the aspect ratio of the liquid meniscus on the device;[24,36] as the wetting properties remain unchanged from run to run, we do not expect any noticeable sensitivity of the size distribution to the volume of liquid dispensed. The weight of the 5 ml peptide solution was taken before nebulization (W_0). After nebulization, solution deposited into each

TABLE II. Size distribution of the nebulized mist of the peptide solution using an NGI.

Stage	% of total mass (%)	D_{50}[a] (μm) at 15 l/min
Induction port + 1	7.14	$\geq$14.1
2	0.96	8.61
3	0.93	5.39
4	12.51	3.3
5	24.37	2.08
6	17.17	1.36
7	15.62	0.98
Micro-orifice collector (MOC)	20.91	<0.98

[a]D_{50} means cut diameter size. It is calculated for each stage. It is the particle diameter for which the efficiency and the penetration are 50% or where half these size particles are captured and half penetrate the collector.

collection cup including the induction port was weighed (W_n), and the mass percentage ($W_n/W_0\%$) of initial weight was calculated. Then, carefully rinsed with 5 ml of water, covered with paraffin film, and left on a shaker overnight for subsequent high performance liquid chromatography (HPLC) testing on the following day. The respirable fraction of the generated aerosol was defined as the total percentage of impacted particles with aerodynamic diameters between 0.98 and 5.39 μm.

D. High performance liquid chromatography (HPLC)

Reverse phase (RP)-HPLC was adopted to determine the peptide concentration in this work. The HPLC system consisted of an LC-20AD pump, DGU-20 A_{5R} degasser, SIL-20A autosampler, and SPD-20AV detector (Shimadzu, Kyoto, Japan). Runs were performed using a Waters XBridge™ C18 column (4.6 × 150 mm, 5 μm; Milford, MA, USA). The wavelength was set at 220 nm and linear gradient elution was utilized. Mobile phases consisting of 0.1% trifluoroacetic acid aqueous solution (A) and acetonitrile with 0.1% trifluoroacetic acid (B) were used with the following gradients: 0.00 min (A 95%–B 5%)-20 min (A 50%–B 50%)-21 min (A 95%–B 5%), under a flow rate of 1 ml/min. The injection volume was fixed at 50 μl. Standard curves were constructed to determine the peptide concentrations in the range of 0–250 mg/l for WW-10 and 0–5000 mg/l for RR-11, RY-11, II-10, MM-10, and LK-8. The peak area A at 220 nm was then plotted linearly against the concentration C of each peptide with r^2 values above 0.9995 (data not shown).

E. Peptide recovery

To determine the concentration recovery of the peptides after nebulization, 200 μl (V_{before}) of peptide solution of fixed concentration C_{before} (500 mg/l) was nebulized in a Falcon tube (Fig. 1(a)). After nebulization, the condensate of peptide mist was collected by centrifugation at 4000 rpm and the volume collected was recorded as V_{after}. The post-nebulized peptide concentration C_{after} was determined by HPLC. The concentration recovery and volume recovery were then calculated as follows:

$$\text{Concentration recovery} = C_{after}/C_{before} \times 100\% = C_{after}/500\,\text{mg/l} \times 100\%, \quad (1)$$

$$\text{Volume recovery} = V_{after}/V_{before} \times 100\% = \text{V}_{\text{after}}/200\mu\text{l} \times 100\%. \quad (2)$$

F. Mass spectrometry (MS) analysis

MS spectra of both nebulized and non-nebulized peptides were obtained using a Synapt G1 mass spectrometer (Waters, Manchester, UK) equipped with an electrospray ion source (ESI). Calibration of the mass spectrometer was first performed in positive ion mode using 200 fmol/μl Glu-fibrinopeptide B (GFP) in 1% formic acid solution in H_2O/CH_3OH (50/50, v/v). Data were acquired from the TOF analyzer from m/z 50 to 1800 Da at a speed of 1 acquisition/s. Peptides samples were then mixed with equal volume of 1% formic acid solution in H_2O/CH_3OH (50/50, v/v) and thereafter infused into the ESI source at a flow rate of 40 μl/min. The capillary voltage was set at +3.5 kV and adjusted for the sampling cone. The source was heated at 80 °C. Nitrogen constituted both the nebulizing and desolvation gases.

G. Minimum inhibition concentration (MIC) measurement

To evaluate the anti-mycobacterial activity of the nebulized peptides, the MICs of the non-nebulized and nebulized peptides against *M. smegmatis* were determined using the broth microdilution method described elsewhere.[37,38] The MIC was defined as the lowest peptide concentrations at which no microbial growth was observed both visually and spectrophotometrically. Briefly, 100 μl of peptide solutions at various concentrations (15.63, 31.25, 62.5, 125, and 250 mg/l) were added to an equal volume of bacterial solution containing approximately 10^5

CFU (colony forming inhibition)/ml per well in a 96-well plate. The plates were then incubated at 37 °C at a shaking speed of 200 rpm. After 72 h, the optical density (OD) at 600 nm was read using a microplate reader (TECAN, Switzerland). Growth media containing only microbial cells were used as the negative control. Each MIC test was carried out in 5 replicates and repeated 3 times.

H. Colony forming inhibition study

The colony forming inhibition activity of the peptide mist generated by the SAW device was evaluated next in order to assess its anti-mycobacterial ability. *M. smegmatis* bacterial solutions ($\sim 3 \times 10^7$ CFU/ml) were diluted by 1000 times and 10 μl of the diluted bacteria solution was spread onto agar plates. 500 μl of RR-11 peptide solutions at different concentrations (MIC, $2 \times$ MIC, and $4 \times$ MIC) were then either sprayed using the SAW device or directly poured onto the agar plates at day 0, day 1, and day 2. On day 3, the bacterial colonies formed were then counted. Pure DI water was used as the control. The study was carried out in 5 replicates and repeated twice.

I. Statistical analysis

Statistical analysis was performed using the statistical software Graphpad (Prism, USA) and quantitative data were expressed as the mean $\pm$ SD. All tests of significance were two-sided, and $p < 0.05$ were considered to be statistically significant.

III. RESULTS

A. Physical integrity of peptides post-nebulization

In order to demonstrate the SAW nebulization platform as an effective peptide delivery system, it is important to first show that the physical integrity of all of the peptides tested is retained post-nebulization. This was confirmed by the results from the MS analysis. A representative MS spectrum of the nebulized and non-nebulized peptide LK-8 is shown in Fig. 3. The two dominant peaks, $(M_W + H)^+$ and $(M_W + 2H)^{2+}$, were observed in the spectra of both nebulized and non-nebulized LK-8. In addition, no degradation peaks were observed in the spectra of the nebulized peptide as compared with non-nebulized peptide spectra, thus suggesting that the SAW nebulization does not lead to peptide denaturation. Similarly, no degradation was seen for RR-11, RY-11, MM-10, II-10, and WW-10 after nebulization (data not shown).

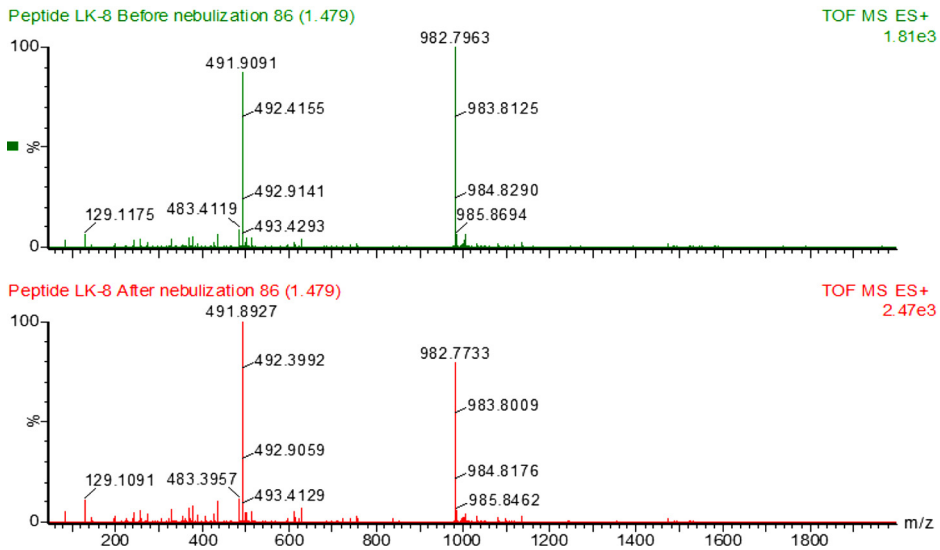

FIG. 3. Mass spectra of peptide LK-8 before (top) and after (bottom) nebulization.

The reason the peptides are not degraded by the SAW nebulization process can be seen from a rough order-of-magnitude comparison between the hydrodynamic stress imposed on the peptide molecules during nebulization and the critical stress required to denature them. The latter can be approximated from a simple polymer chain stretching model under elongational flow, wherein the critical stress required for unfolding by breaking the peptide bond is given by[39]

$$\tau_c \approx \frac{\Delta}{\pi d^2 N^{4/3} (3v_b/8\pi)^{1/3}}, \tag{3}$$

in which $d \approx 3.8\,\text{Å}$ is the interstitial distance between the centers of two consecutive spherical beads in the chain of N beads (or residues), $v_b \approx 1.5 \times 10^{-28}\ \text{m}^3$ is the average volume occupied by a bead, and $\Delta = \Delta G/N$ (assuming that the peptide possesses native-like stability to begin with), wherein $\Delta G \approx 40\,\text{kJ/mol}$ is the thermodynamic stability of the folded state[40] such that $\Delta \approx 7 \times 10^{-21}$ J/residue. It then follows from Eq. (3) that stresses on the order of 1 MPa are required to denature a peptide molecule. It is therefore unsurprising that peptides as well as proteins are often damaged by conventional ultrasonic nebulizers, given the typical 1–100 MPa pressures that biomolecules are subjected to[41] upon collapse of the cavitational bubbles required to generate aerosolization in such nebulizers. In contrast, the elongational stress exerted by the substrate acceleration due to the SAW can be estimated from

$$\tau_{SAW} \approx \mu \frac{\Delta U}{\beta^{-1}}, \tag{4}$$

where μ is the fluid viscosity and

$$\beta^{-1} \approx \left(\frac{\mu}{\pi \rho f}\right)^{1/2} \tag{5}$$

is the viscous penetration depth over which the sound energy that leaks into the fluid characteristically decays,[42] with ρ being the fluid density and f is the SAW frequency. Given an upper limit of 1 m/s in the SAW substrate displacement velocity U, a conservative estimate of the stress imposed on the peptide by the SAW during nebulization is on the order of 0.01 MPa—considerably smaller than the critical stress required to denature the peptides.

B. *In vitro* airway deposition characteristics

To ascertain the suitability of the aerosol peptide delivery for inhalation therapy, we examined the *in vitro* airway deposition characteristics of the peptide aerosols using an NGI, results of which tabulated in Table II show that approximately 70% of the peptide aerosols fell within the size range of 0.98–5.39 μm, which is ideal for deep lung deposition, as aerosols fall in 1–5 μm aerodynamic range are demonstrated as respirable fraction.[43]

C. Recovery study of peptide nebulization

In order to assure accurate dosing, the impact of SAW nebulization on peptide concentration and loss of volume on device was assessed by a recovery test in which the post-nebulization peptide concentration and volume recovery were determined for each peptide. As shown in Table III, both the concentration and the volume recoveries across all peptides were significantly higher than 90% ($p < 0.05$). Additionally, concentration recovery and volume recovery of different peptides were not statistically different ($p > 0.05$).

D. Therapeutic efficacy of peptides post-nebulization

In order to determine whether the anti-mycobacterial activity was compromised during the nebulization process, we first carried out MIC assay against *M. smegmatis* using both non-nebulized

TABLE III. Summary of concentration and volume recoveries of each peptide after nebulization.

	Concentration recovery	Volume recovery
RR-11	93.35 ± 3.11	95.75 ± 2.07
RY-11	94.11 ± 2.71	96.70 ± 1.30
LK-8	93.90 ± 2.44	95.17 ± 1.63
MM-10	91.59 ± 1.01	95.60 ± 1.92
II-10	92.89 ± 0.98	95.30 ± 1.44
WW-10	92.27 ± 1.25	95.33 ± 0.75

and nebulized peptides. As seen in Table IV, the anti-mycobacterial activity of the nebulized peptides remained unaltered as compared with the non-nebulized peptides, evident from the effective minimum inhibitory concentrations against *M. smegmatis* of 62.5–125 mg/l which are in agreement with the previously published data.[30,31] To further assess the anti-mycobacterial activity of the peptide mist generated by the SAW device, we also compared the colony forming inhibition activity resulting from direct spraying of the nebulized peptide mist with the direct addition of the non-nebulized peptide solution onto the agar plates. As shown in Fig. 4, application of peptides in the form of both the nebulized mist and the solution significantly inhibited the bacterial colony formation at concentrations equivalent to MIC, $2 \times$ MIC, and $4 \times$ MIC as compared with the controls ($p < 0.05$). No statistical difference was observed between the inhibition efficiencies of the peptide mist and solution, indicating the retention of its bioactivity after nebulization.

IV. DISCUSSION

The maintenance of bioactivity and physical integrity of nebulized peptide is an essential pre-requisite for effective pulmonary delivery of therapeutic peptides. The SAW platform was found to be a promising avenue to produce peptide aerosol without compromising the structural integrity and anti-mycobacterial activity of these model peptides as shown in the MS, MIC, and colony forming inhibition results of the present study. In addition, the airway deposition characteristic is critical to ascertain the suitability of the peptide aerosol for inhalation therapy. It is widely accepted that macromolecules tend to be absorbed at greater rates when they are delivered to the deep lung as compared with the central airways.[44,45] As such, it is desirable that the peptide aerosols fall within the 1 to 5 μm aerodynamic diameter range optimal for deep lung deposition[43] since aerosols with diameters below 1 μm tend to be exhaled, whereas the majority of aerosols with diameters above 5 μm tend to deposit in the upper respiratory tract. The NGI results tabulated in Table II show that approximately 70% of the peptide aerosols fall within the size range of 1–5 μm, therefore constituting a respirable fraction for the SAW nebulized peptide aerosol that is comparable to 60% respirable peptide aerosol generated by dry powder inhaler.[10] Currently used nebulizers and inhalers typically provide 30%–40%[46] lung deposition *in vivo* and animal study could be performed in the future using SAW platform for further comparison. Furthermore, the concentration recovery of the nebulized peptides is significantly higher than 90% which indicates that peptide concentrations were not significantly affected by nebulization, and minimal volume of peptide solution was wasted during the nebulization. Additionally, the recoveries of different peptides were not statistically different, which indicates that the concentration recovery is insensitive to the type of peptide. As such, SAW nebulization

TABLE IV. MICs of peptides against *M. smegmatis* before/after nebulization.

Peptides		RR-11	RY-11	LK-8	MM-10	II-10	WW-10
MIC (mg/l)	Before	125	125	125	62.5	62.5	62.5
	After	125	125	125	62.5	62.5	62.5

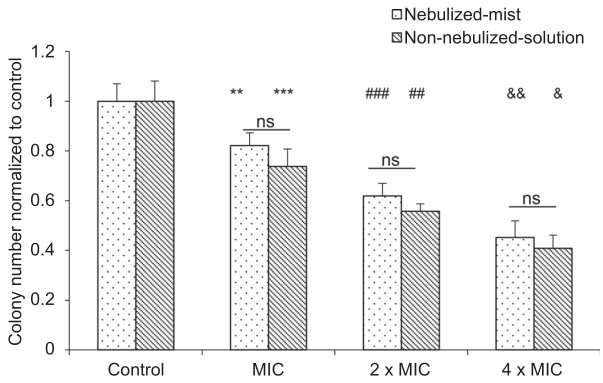

FIG. 4. The colony number of each group is normalized to that of the control group after application of either the peptide mist generated by the SAW nebulization device or the peptide solution directly poured onto agar plates that has previously been spread with *M. smegmatis*. For the "nebulized-mist" group, "**" indicates $p < 0.01$ when compared with the control group; "###" indicates $p < 0.001$ when compared with $1 \times$ MIC; and "&&" indicates $p < 0.01$ when compared with $2 \times$ MIC; For the "non-nebulized-solution" group, "***" indicates $p < 0.001$ when compared with the control group; "##" indicates $p < 0.01$ when compared with $1 \times$ MIC; "&" indicates $p < 0.05$ when compared with $2 \times$ MIC; and "ns" indicates a result that is not statistically significant between the nebulized-mist and the non-nebulized-solution groups.

platform constitutes a generic and versatile platform that can be potentially developed for the effective delivery of a wide range of therapeutic peptides. Further optimization and validation could facilitate in developing an SAW nebulization system for the administration of therapeutic peptides that are sufficiently energy efficient, hence allowing its miniaturization into a portable, cost-effective platform.

V. CONCLUSION

By verifying that the nebulized peptides retained their structural integrity as well as bioactivity, we thus demonstrate its potential as an effective pulmonary delivery system for therapeutic peptides, which could therefore constitute a very effective tool for the treatment of microbial respiratory infections, such as pneumonia, Legionnaires' disease, and tuberculosis. Other possible applications include pulmonary delivery of therapeutic peptides for the treatment of asthma, cystic fibrosis, and lung cancer, and the delivery of systemically acting peptides for the treatment of diseases such as diabetes and cancers.

ACKNOWLEDGMENTS

The authors acknowledge the research funding and facilities provided by the National University of Singapore (NUS). The research was also supported by the Singapore Ministry of Health's National Medical Research Council under its Individual Research Grant Scheme (NMRC/1298/2011) and the MOE ACRF Tier 1 grant (R148000200112) awarded to P.L.R.E. In addition, Y.W. and J.S.K. are grateful for the NUS President's Graduate Fellowship and A.R.R. for a Churchill Fellowship from the Winston Churchill Memorial Trust. L.Y.Y. is thankful for an Australian Research Council Future Fellowship (FT130100672).

[1]Z. Y. Ong, N. Wiradharma, and Y. Y. Yang, Adv. Drug Delivery Rev. **78**, 28 (2014).
[2]L. M. Rossi, P. Rangasamy, J. Zhang, X. Q. Qiu, and G. Y. Wu, J. Pharm. Sci. **97**, 1060 (2008).
[3]Y. Huang, N. Wiradharma, K. Xu, Z. Ji, S. Bi, L. Li, Y. Y. Yang, and W. Fan, Biomaterials **33**, 8841 (2012).
[4]Y. Lan, J. T. Lam, G. K. Siu, W. C. Yam, A. J. Mason, and J. K. Lam, Tuberculosis **94**, 678 (2014).
[5]B. Deslouches, J. D. Steckbeck, J. K. Craigo, Y. Doi, J. L. Burns, and R. C. Montelaro, Antimicrob. Agents Chemother. **59**, 1329 (2015).
[6]X. Li, M. Yu, W. Fan, Y. Gan, L. Hovgaard, and M. Yang, Expert Opin. Drug Delivery **11**, 1435 (2014).
[7]M. E. Falagas, I. I. Siempos, P. I. Rafailidis, I. P. Korbila, E. Ioannidou, and A. Michalopoulos, Respir. Med. **103**, 707 (2009).
[8]M. Sakagami, Ther. Delivery **4**, 1511 (2013).
[9]M. Grant and A. Leone-Bay, Ther. Delivery **3**, 981 (2012).
[10]M. Irngartinger, V. Camuglia, M. Damm, J. Goede, and H. W. Frijlink, Eur. J. Pharm. Biopharm. **58**, 7 (2004).

[11]A. Leone-Bay, M. Grant, S. Greene, G. Stowell, S. Daniels, A. Smithson, S. Villanueva, S. Cope, K. Carrera, S. Reyes, and P. Richardson, Diabetes, Obes. Metab. **11**, 1050 (2009).
[12]P. P. Nadkarni, R. M. Costanzo, and M. Sakagami, Diabetes, Obes. Metab. **13**, 408 (2011).
[13]D. Hubert, S. Leroy, R. Nove-Josserand, M. Murris-Espin, L. Mely, S. Dominique, B. Delaisi, P. Kho, and J. M. Kovarik, J. Cystic Fibrosis **8**, 332 (2009).
[14]American Thoracic Society and Infectious Diseases Society of America, Am. J. Respir. Crit. Care Med. **171**, 388 (2005).
[15]A. Misra, A. J. Hickey, C. Rossi, G. Borchard, H. Terada, K. Makino, P. B. Fourie, and P. Colombo, Tuberculosis **91**, 71 (2011).
[16]F. Qian, N. Mathias, P. Moench, C. Chi, S. Desikan, M. Hussain, and R. L. Smith, Int. J. Pharm. **366**, 218 (2009).
[17]L. Y. Yeo, J. R. Friend, M. P. McIntosh, E. N. Meeusen, and D. A. Morton, Expert Opin. Drug Delivery **7**, 663 (2010).
[18]J. Friend and L. Y. Yeo, Rev. Mod. Phys. **83**, 647 (2011).
[19]L. Y. Yeo and J. R. Friend, Biomicrofluidics **3**, 012002 (2009).
[20]X. Ding, P. Li, S.-C. S. Lin, Z. S. Stratton, N. Nama, F. Guo, D. Slotcavage, X. Mao, J. Shi, F. Costanzo, and T. J. Huang, Lab Chip **13**, 3626 (2013).
[21]L. Y. Yeo and J. R. Friend, Annu. Rev. Fluid Mech. **46**, 379 (2014).
[22]G. Destgeer and H. J. Sung, Lab Chip **15**, 2722 (2015).
[23]M. Kurosawa, T. Watanabe, A. Futami, and T. Higuchi, Sens. Actuators, A **50**, 69 (1995).
[24]A. Qi, L. Y. Yeo, and J. R. Friend, Phys. Fluids **20**, 074103 (2008).
[25]A. Rajapaksa, A. Qi, L. Y. Yeo, R. Coppel, and J. R. Friend, Lab Chip **14**, 1858 (2014).
[26]S. R. Heron, R. Wilson, S. A. Shaffer, D. R. Goodlett, and J. M. Cooper, Anal. Chem. **82**, 3985 (2010).
[27]J. Ho, M. K. Tan, D. B. Go, L. Y. Yeo, J. R. Friend, and H.-C. Chang, Anal. Chem. **83**, 3260 (2011).
[28]Y. Huang, S. H. Yoon, S. R. Heron, C. D. Masselon, J. S. Edgar, F. Tureček, and D. R. Goodlett, J. Am. Soc. Mass Spectrom. **23**, 1062 (2012).
[29]A. Qi, J. R. Friend, L. Y. Yeo, D. A. Morton, M. P. McIntosh, and L. Spiccia, Lab Chip **9**, 2184 (2009).
[30]J. S. Khara, Y. Wang, X. Y. Ke, S. Liu, S. M. Newton, P. R. Langford, Y. Y. Yang, and P. L. Ee, Biomaterials **35**, 2032 (2014).
[31]Y. Wang, X. Y. Ke, J. S. Khara, P. Bahety, S. Liu, S. V. Seow, Y. Y. Yang, and P. L. Ee, Biomaterials **35**, 3102 (2014).
[32]A. Qi, L. Yeo, J. Friend, and J. Ho, Lab Chip **10**, 470 (2010).
[33]United States Pharmacopeia, Vol. 28, General Chapter ⟨601⟩ (United States Pharmacopeial Convention, Rockville, MD, 2005).
[34]European Pharmacopoeia 7.1 (Council of Europe, Strasbourg, France, 2011), Section 2.9.18, pp. 274–284.
[35]V. A. Marple, B. A. Olson, K. Santhanakrishnan, D. L. Roberts, J. P. Mitchell, and B. L. Hudson-Curtis, J. Aerosol Med. **17**, 335 (2004).
[36]D. J. Collins, O. Manor, A. Winkler, H. Schmidt, J. R. Friend, and L. Y. Yeo, Phys. Rev. E **86**, 056312 (2012).
[37]H. Wang, K. Xu, L. Liu, J. P. Tan, Y. Chen, Y. Li, W. Fan, Z. Wei, J. Sheng, Y. Y. Yang, and L. Li, Biomaterials **31**, 2874 (2010).
[38]L. Liu, K. Xu, H. Wang, P. K. J. Tan, W. Fan, S. S. Venkatraman, L. Li, and Y. Y. Yang, Nat. Nanotechnol. **4**, 457 (2009).
[39]J. Jaspe and S. J. Hagen, Biophys. J. **91**, 3415 (2006).
[40]R. B. Martin, Biopolymers **45**, 351 (1998).
[41]E. Herbert, S. Balibar, and F. Caupin, Phys. Rev. E **74**, 041603 (2006).
[42]O. Manor, L. Y. Yeo, and J. R. Friend, J. Fluid Mech. **707**, 482 (2012).
[43]J. C. Sung, B. L. Pulliam, and D. A. Edwards, Trends. Biotechnol. **25**, 563 (2007).
[44]S. Sangwan, J. M. Agosti, L. A. Bauer, B. A. Otulana, R. J. Morishige, D. C. Cipolla, J. D. Blanchard, and G. C. Smaldone, J. Aerosol Med. **14**, 185 (2001).
[45]V. Codrons, F. Vanderbist, B. Ucakar, V. Preat, and R. Vanbever, J. Pharm. Sci. **93**, 1241 (2004).
[46]A. E. Rajapaksa, J. J. Ho, A. Qi, R. Bischof, T. H. Nguyen, M. Tate, D. Piedrafita, M. P. McIntosh, L. Y. Yeo, E. Meeusen, R. L. Coppel, and J. R. Friend, Respir. Res. **15**, 60 (2014).